Fast Frequency Sweep Analysis of Passive Miniature RF Circuits Based on Analytic Extension of Eigenvalues

Hongliang Li, *Graduate Student Member, IEEE*, Jian-Ming Jin, *Fellow, IEEE*, Douglas R. Jachowski, *Member, IEEE*, and Robert B. Hammond, *Life Member, IEEE*

***Abstract*— A fast frequency sweep approach based on analytic extension of eigenvalues (AEE) is presented and investigated for an efficient analysis of miniature passive RF circuits. In this approach, an eigenvalue decomposition is performed to the Z-parameters of the circuit components at one or a few frequencies, and analytic extension is applied to obtain the eigenvalues at all other frequencies within the band of interest. For electrically small circuit components, the frequency-independent characteristic inductances and capacitances, as well as the frequency-dependent resistances, are extracted from the eigenvalues at the sampling frequencies. The extracted characteristic parameters are then used to approximate the Z- and Y-parameters and predict the responses of the circuit over the entire frequency band. The accuracy of this approach is evaluated by comparing it with the results from a full-wave analysis. It is found that the proposed AEE is very accurate with a relative error of less than 1% for miniature RF circuits whose electrical sizes are smaller than one tenth of the wavelength and is more general and powerful than the one based on lumped equivalent circuits.**

***Index Terms*— Eigenmode analysis, fast frequency sweep, quasi-static analysis, RF circuit modeling.**

I. Introduction

FAST and accurate numerical modeling is critical for the design and optimization of novel RF circuits and devices. This is particularly true when artificial intelligence algorithms, such as machine learning, are employed for such design and optimization because these algorithms require a large amount of data for training and validation. For RF circuits and devices, numerical methods such as the finite-element method (FEM) and the moment method (MoM), have been very well developed for accurate numerical modeling. They are most efficient when performing a single-frequency analysis; however, they become time consuming for a frequency sweep analysis over a broad frequency band because they require solving a large numerical system repeatedly at many frequencies. To alleviate this problem, a variety of fast frequency sweeping techniques have been developed in the past, which were based on either physical or mathematical models.

The most straightforward physical-based fast frequency sweeping technique is the well-known lumped equivalent circuit (LEC) method [1]–[4], which models a small distributive RF circuit in terms of lumped equivalent elements with their capacitances, inductances, and resistances extracted from a quasi-static or full-wave numerical analysis. With the extracted lumped elements, the behavior of the RF circuit can be predicted over the desired frequency band. However, this approach has a disadvantage that the equivalent circuit model can be very complicated if the number of ports in the RF device is large, and the calculation and extraction of the characteristic parameters for each element in the model can be tedious. These challenges greatly limited the application of the LEC method.

The more powerful and generally applicable fast frequency sweeping techniques are mathematical based, such as the model-based parameter extraction (MBPE) [5], [6], the asymptotic waveform evaluation (AWE) [7]–[9], the Padé via Lanczos (PVL) [10]–[13], and the solution space projection (SSP) [14]–[16] methods. These methods employ mathematical functions such as rational functions to expand the frequency response of an RF circuit and then determine the expansion coefficients based on a full-wave numerical analysis at sampling frequencies. Because of their high efficiency and generality, the mathematical-based frequency sweeping techniques have been widely implemented in commercial simulation software. However, they are unable to produce a physical model such as an equivalent circuit model that can provide a direct physical insight for circuit designers and they have to be implemented in a specific numerical algorithm.

In this article, we present a new fast frequency sweeping technique based on analytic extension of eigenvalues (AEE) for an efficient analysis of miniature passive RF circuits over a broad frequency band. The AEE applies an eigenvalue analysis to the Z-parameters of an RF circuit at one or two frequency points and then extend the eigenvalues to other frequency points within the desired frequency band via analytic extension through a functional equation. The functional equation can

Manuscript received May 9, 2020; revised July 11, 2020, August 27, 2020, and September 20, 2020; accepted September 28, 2020. Date of publication October 28, 2020; date of current version January 5, 2021. *(Corresponding author: Jian-Ming Jin.)*

Hongliang Li and Jian-Ming Jin are with the Center for Computational Electromagnetics, Department of Electrical and Computer Engineering, University of Illinois at Urbana–Champaign, Urbana, IL 61801 USA (e-mail: hl23@illinois.edu; j-jin1@illinois.edu).

Douglas R. Jachowski and Robert B. Hammond are with Resonant Inc., Goleta, CA 93117 USA (e-mail: djachowski@resonant.com; bhammond@resonant.com).

Color versions of one or more of the figures in this article are available online at https://ieeexplore.ieee.org.

Digital Object Identifier 10.1109/TMTT.2020.3031584

be constructed based on an RLC circuit for each eigenvalue, from which the characteristic capacitance, inductance, and resistance can be extracted. With the eigenvalues calculated at all frequencies, the Z- or Y-parameters of the RF circuit can be calculated based on the expansion in terms of the corresponding eigenvectors; thus, the characteristics of the circuit over the frequency band can be predicted efficiently.

Compared to the physical- and mathematical-based fast frequency sweeping techniques mentioned earlier, the AEE method can be considered as a hybrid technique and enjoys three advantages. First, unlike the physical-based techniques, which are usually limited by the ability to construct a physical model that can accurately mimic the true characteristics of the original RF circuit, the AEE is a mathematical approach, which does not rely on an explicit equivalent circuit model and thus makes the method more generally applicable. Second, unlike the mathematical-based techniques, the AEE can automatically yield an LEC model, which not only provides important physical insights but also can be directly incorporated into a circuit analysis if necessary. Third, different from the mathematical based techniques, which are applied to the original numerical system of the employed numerical algorithm, the AEE applies to the calculated Z-parameters directly, so it is independent of the specific numerical algorithm. Furthermore, the dimension of the eigenvalue problem in the AEE is equal to the number of ports in the circuit, which is usually very small and thus makes the AEE computationally inexpensive.

We must note that although the proposed AEE method bears certain similarities to the recently developed characteristic mode analysis (CMA), which has been applied successfully to antenna analysis and design [17]–[29], the two are different both in terms of the mathematical formulation and final objectives. The CMA is formulated from integral equations and solves a generalized eigenvalue problem for the impedance matrix resultant from the MoM [17], [18]. The resulting eigenvectors represent the characteristic currents that can naturally exist on the antenna and their superposition can form the true current distribution. Since the corresponding radiation pattern can be obtained for each mode, the CMA can then be used to synthesize the desired radiation pattern by judiciously exciting necessary eigenmodes on the antenna. In the AEE for RF circuit analysis, the key idea is to provide a fast frequency sweeping technique to compute the frequency response of an RF circuit efficiently based on the AEE from the sampling frequency points to all other points via a functional equation. The types of eigenvalue problems involved and the dimensions of the eigenvalue problems are very different in the CMA and AEE.

The proposed AEE is also different from the modal analysis commonly used in microwave engineering for analyzing the crosstalk between coupled lines based on telegrapher equations [30]–[32]. This modal analysis first extracts the inductance and capacitance matrices, $[L]$ and $[C]$, from a static analysis, and then performs an eigenvalue decomposition to matrices $[L][C]$ and $[C][L]$ to obtain the modal characteristic impedance and admittance, which is only applicable to transmission line systems consisting of N conductors. Although both approaches apply an eigenvalue decomposition, the AEE method decomposes the extracted Z-parameters directly into eigenmodes and is applicable to any N-port RF circuits.

The objective of this article is to present the AEE method and investigate its capability for a fast frequency sweep analysis of RF circuits. Although the AEE method is a relatively general approach, we will limit to the case where the RF circuits are electrically small or the frequency band of interest is relatively low. For such a case, the characteristic capacitance and inductance in the functional equation and the eigenvectors can all be assumed invariant over the frequency band. We shall refer it to as the quasi-static AEE. In this article, we first present the formulation of the quasi-static AEE and then conduct an extensive investigation on its accuracy. Finally, we consider and discuss the modeling of various losses and draw a conclusion.

II. Formulation

The proposed AEE can be used with any full-wave analysis method. Here, we describe briefly a full-wave analysis based on the FEM [33], which is used to produce all the results in this article. Consider a circuit excited by a current density $\mathbf{J}_{\text{imp}}$, and the electric field $\mathbf{E}$ is governed by the wave equation

$$\nabla \times (\nu_r \nabla \times \mathbf{E}) - \mathrm{k}_0^2 \varepsilon_r \mathbf{E} = -\mathrm{j}\omega\mu_0 \mathbf{J}_{\text{imp}} \tag{1}$$

where ε_r denotes the relative permittivity and $\nu_r = 1/\mu_r$ with μ_r being the relative permeability. Testing the equation with a weighting function $\mathbf{W}_i$ and integrating over the solution domain [33], we obtain the weak-form representation of (1) as

$$\iiint_V \left[(\nabla \times \mathbf{W}_i) \cdot \nu_r (\nabla \times \mathbf{E}) - \mathrm{k}_0^2 \varepsilon_r \mathbf{W}_i \cdot \mathbf{E}\right] \mathrm{d}V = -\mathrm{j}\omega\mu_0 \iiint_V \mathbf{W}_i \cdot \mathbf{J}_{\text{imp}} \mathrm{d}V \tag{2}$$

where it is assumed that the circuit is enclosed by a perfect electrically conducting (PEC) or perfect magnetically conducting (PMC) surface. Other surfaces, such as absorbing and impedance surfaces, can be modeled with a simple modification to the formulation.

To discretize (2), we first expand the electric field using the curl-conforming basis functions as

$$\mathbf{E} = \sum_j \mathbf{N}_j e_j \tag{3}$$

where $\mathbf{N}_j$ denotes the edge-based vector basis functions. The tree–cotree splitting algorithm [34]–[36] is applied to enforce the gauge condition and avoid the low-frequency breakdown problem. By following Galerkin's method, (2) can be discretized to yield a linear algebraic system as:

$$[K]\{e\} = \{b\} \tag{4}$$

where

$$[K]_{ij} = \iiint_V \left[(\nabla \times \mathbf{N}_i) \cdot \nu_r \left(\nabla \times \mathbf{N}_j\right) - \mathrm{k}_0^2 \varepsilon_r \mathbf{N}_i \cdot \mathbf{N}_j\right] \mathrm{d}V \tag{5}$$

$$\{b\}_i = -\mathrm{j}\omega\mu_0 \iiint_V \mathbf{N}_i \cdot \mathbf{J}_{\text{imp}} \mathrm{d}V. \tag{6}$$

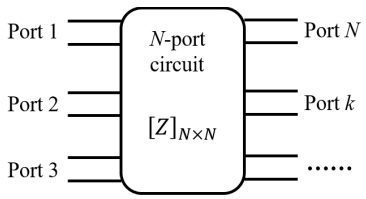

Fig. 1. N-port circuit network and Z-matrix description.

For a line current source, $\{b\}$ is given by

$$\{b\}_i = -\mathrm{j}\omega\mu_0 I \int_C \mathbf{N}_i \cdot \hat{l}\mathrm{d}l \tag{7}$$

where $\hat{l}$ denotes the direction of the current. By solving (4) for a given frequency, we obtain an accurate full-wave solution to the electric field. To extract the Z-parameters, the circuit is excited at one port a time with a lumped element current source. By exciting the ports in turn, the voltage and current values at all the ports can be readily calculated and transformed into the Z-parameters.

Once the Z-parameters are obtained with a full-wave analysis at a chosen frequency, the AEE is applied to perform an eigenvalue analysis. However, different from the CMA, where a generalized eigenvalue problem is solved by splitting the real and imaginary parts of the MoM impedance matrix to guarantee the orthogonality of the radiation patterns, here, a standard eigenvalue problem is solved to diagonalize the circuit's Z-parameters as this would provide a more straightforward insight into the physical meaning of the eigenvalues. Furthermore, by diagonalizing Z-parameters, complex eigenvalues are obtained whose values can be modeled as an impedance of a lumped circuit model where the characteristic resistance and reactance have different variations with frequency and can be analyzed separately. Otherwise, if a generalized eigenvalue problem is formulated as is done in the CMA, the frequency behavior of the eigenvalues becomes difficult to model and certain approximations have to be employed for the extension to other frequencies [37].

Consider an N-port circuit as shown in Fig. 1, and the Z-parameters are defined as

$$[Z]\{I\} = \{V\} \tag{8}$$

where $[Z] = [R] + \mathrm{j}[X]$ is the N-port impedance matrix, $\{I\}$ is the current vector flowing into the ports, and $\{V\}$ is the voltage vector on the ports. Now, consider the standard eigenvalue problem

$$[Z]\{\upsilon_n\} = \lambda_n\{\upsilon_n\} \tag{9}$$

where λ_n denotes the eigenvalues and $\{\upsilon_n\}$ denotes the corresponding eigenvectors. Since $[Z]$ is not Hermitian, λ_n and $\{\upsilon_n\}$ may be complex. However, for reciprocal circuits, the impedance matrix is symmetric, and we have the orthogonality relations

$$\{\upsilon_m\}^{\mathrm{T}}\{\upsilon_n\} = \delta_{mn}. \tag{10}$$

When $\{\upsilon_n\}$ are calculated, any current vector $\{I\}$ can then be represented by an eigen expansion using eigenvectors $\{\upsilon_n\}$ as the basis functions

$$\{I\} = \sum_n \alpha_n\{\upsilon_n\}. \tag{11}$$

Depending on whether the circuit is excited by a current or voltage source, the coefficients α_n can be determined by utilizing the orthogonality from (10) in a slightly different manner. For example, when the Y-parameters are of interest, the voltage excitation $\{V_{\mathrm{src}}\}$ should be applied by definition. Substituting (11) into (8) and testing it with $\{\upsilon_m\}$ yields

$$\sum_n \alpha_n\{\upsilon_m\}^{\mathrm{T}}[Z]\{\upsilon_n\} = \{\upsilon_m\}^{\mathrm{T}}\{V_{\mathrm{src}}\}. \tag{12}$$

Because of the orthogonality relationship (10), (12) reduces to

$$\alpha_n = \frac{\{\upsilon_n\}^{\mathrm{T}}\{V_{\mathrm{src}}\}}{\lambda_n}. \tag{13}$$

If the Z-parameters are to be computed, the current source should be impressed instead. The derivation of the coefficients then becomes much easier, and one only needs to take the inner product of (11) with $\{\upsilon_m\}$, which gives

$$\alpha_n = \{\upsilon_n\}^{\mathrm{T}}\{I_{\mathrm{src}}\}. \tag{14}$$

Next, we examine the physical meaning of the eigenvalues to formulate a functional equation to extend the eigenvalues from one or two sampling frequencies to all other frequencies within the frequency band of interest. Since the standard eigenvalue problem diagonalizes the impedance matrix into

$$[Z] = \begin{bmatrix} \lambda_1 & & & \\ & \lambda_2 & & \\ & & \ddots & \\ & & & \lambda_N \end{bmatrix} \tag{15}$$

the eigenvalue λ_n corresponds to the impedance for the nth eigenmode. In the antenna community, it is found that the input impedance for each characteristic mode can be represented by a series RLC model [38]–[40]. Therefore, it is intuitive to express the functional equation for the AEE as

$$\lambda_n = R_n + \mathrm{j}\omega L_n + \frac{1}{\mathrm{j}\omega C_n} \tag{16}$$

where R_n, L_n, and C_n are the characteristic resistance, inductance, and capacitance, respectively. Although this representation is purely mathematical, it implicitly provides an LEC model and gives physical meaning to the eigenvalues. However, it should be pointed out that λ_n is not an input impedance at any port although the impedance of a lumped circuit is used to express the eigenvalues. Instead, the eigenvalue together with its corresponding eigenvector contributes to the self-impedance and mutual impedance between all ports for each mode. By superposing the contributions of all modes, the Z-parameters can be obtained. For RF circuits that are electrically very small, a quasi-static approximation can be made in which L_n and C_n as well as the eigenvectors $\{\upsilon_n\}$ are assumed to be frequency independent over the frequency band [23]. Note that the characteristic resistance R_n is not

necessarily constant. However, over the frequency band where the quasi-static analysis is valid, the behavior of R_n as a function of frequency is supposed to be *a priori* knowledge. Specifically, the frequency-dependent resistance varies exponentially as $R_n \sim f^{\beta}$. For example, the sheet resistance from the skin effect gives $\beta = 0.5$, and the resistance due to the dielectric loss gives $\beta = -1$.

Once the eigenvalues at two frequency points are obtained by the AEE, the imaginary parts can be taken to solve for the constant L_n and C_n based on (16). Through extensive numerical experiments, it is found that for electrically small circuits, all modes are either capacitively or inductively dominant, and there are no zero crossings and, therefore, no resonances. A further approximation can be made to reduce the computation to one single-frequency point [37]. For an eigenvalue with a positive imaginary part, it is an inductively dominant mode and the inductance L_n contributes more to the total impedance. Therefore, the functional equation (16) can be approximated as

$$\mathrm{Im}(\lambda_n) \approx \omega L_n. \tag{17}$$

Similarly, for an eigenvalue with a negative imaginary part, the capacitance C_n dominates and only the capacitive term is to be considered as

$$\mathrm{Im}(\lambda_n) \approx -\frac{1}{\omega C_n}. \tag{18}$$

Utilizing the results from two frequency points to consider both L_n and C_n will improve the accuracy, and hence, a tradeoff has to be made between the accuracy and the cost. Once R_n, L_n, and C_n are determined, the eigenvalues at all frequencies can be predicted by (16)–(18).

Once the eigenvalues are computed at all the frequency points, the Z- and Y-parameters can be calculated very efficiently. By definition, Z_{ij} can be found by driving port j with the current $I_j = 1$, with all other ports open, and measuring the voltage at port i, so that

$$Z_{ij} = \left.\frac{V_i}{I_j}\right|_{I_k=0 \text{ for } k\neq j} = V_i|_{I_j=1,\ I_k=0 \text{ for } k\neq j}. \tag{19}$$

Therefore, we first excite port j and leave all other ports open-circuited, which gives $\{I_{\mathrm{src}}^{(j)}\} = [0\ldots0,1,0,\ldots,0]^{\mathrm{T}}$ with only the jth element to be one and all others to be zero. By substituting the current source vector $\{I_{\mathrm{src}}^{(j)}\}$ into the modal expansion in (11), the voltages on the ports can be computed as

$$\begin{aligned}\left\{V^{(j)}\right\} &= [Z]\left\{I_{\mathrm{src}}^{(j)}\right\} = \sum_n \alpha_n^{(j)}[Z]\{v_n\} \\ &= \sum_n \alpha_n^{(j)}\lambda_n\{v_n\}\end{aligned} \tag{20}$$

where $\alpha_n^{(j)}$ are obtained by (14) as $\alpha_n^{(j)} = \{v_n\}_j^{\mathrm{T}}$. Z_{ij} can finally be written in a compact form as

$$[Z] = \sum_n \lambda_n\{v_n\}\{v_n\}^{\mathrm{T}}. \tag{21}$$

Similarly, to compute Y_{ij}, which are defined as

$$Y_{ij} = I_i|_{V_j=1,\ V_k=0 \text{ for } k\neq j} \tag{22}$$

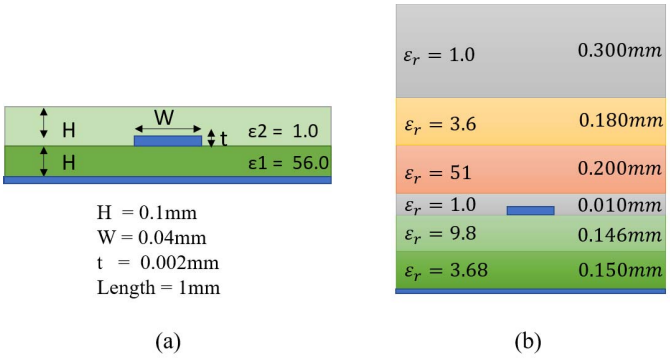

Fig. 2. Test problems for the quasi-static AEE. (a) Two-layer microstrip line. (b) Five-layer microstrip line.

we can set the voltage source to $\{V_{\mathrm{src}}^{(j)}\} = [0\ldots0,1,0,\ldots,0]^{\mathrm{T}}$ with only the jth element to be one and all others to be zero and then find the modal solution of the current at port i. Finally, we have

$$[Y] = \sum_n \frac{\{v_n\}\{v_n\}^{\mathrm{T}}}{\lambda_n}. \tag{23}$$

In (21) and (23), $\{v_n\}$ represents the current flowing into the ports for the nth mode. The eigenvalue together with the eigenvector gives the self-impedance and mutual impedance or admittance for each mode.

III. Numerical Results

In this section, we present the comparison between the quasi-static AEE and full-wave solutions for several testing problems to investigate the range of validity and errors of the AEE-based quasi-static analysis.

A. Single Frequency Versus Two Frequencies

Two test problems are designed to examine the behavior of the eigenvalues in the quasi-static AEE and compare the accuracy between the single- and two-frequency computations. The first consists of a conducting strip, which is 0.04 mm wide, 0.002 mm thick, and 1.0 mm long, and is embedded in a two-layer medium shown in Fig. 2(a). The whole structure is bounded by a conducting shield, which is 0.36 mm wide. The conducting strip is excited by a 1.0-A current source at one end and terminated by a 50-Ω resistor at the other end. The second one consists of the same conducting strip as in the first problem, but now, it is embedded in a five-layer medium, as shown in Fig. 2(b). Again, the conducting strip is excited by a 1.0-A current source at one end and terminated by a resistor with $R = 50\ \Omega$ at the other end. For both problems, the desired frequency band is from 400 MHz to 4 GHz.

Figs. 3 and 4 show the imaginary parts of the eigenvalues for all the modes in the two problems. Since these are two-port lossless circuits, the real parts that represent the resistance can be neglected. For the eigenvalues with a positive imaginary part, the inductive component dominates, which has a linear behavior as the function of frequency; hence, the approximation in (17) is applicable. For the eigenvalues whose imaginary

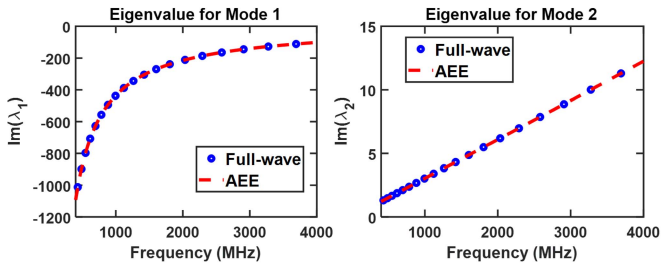

Fig. 3. Imaginary parts of the eigenvalues versus frequency for test problem 1.

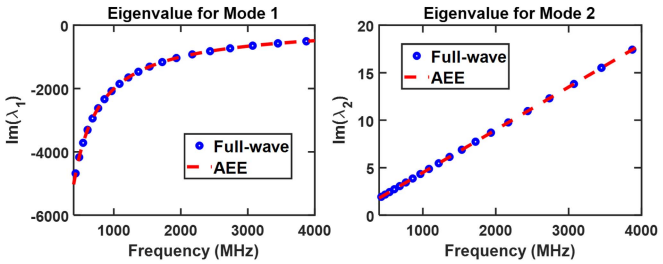

Fig. 4. Imaginary parts of the eigenvalues versus frequency for test problem 2.

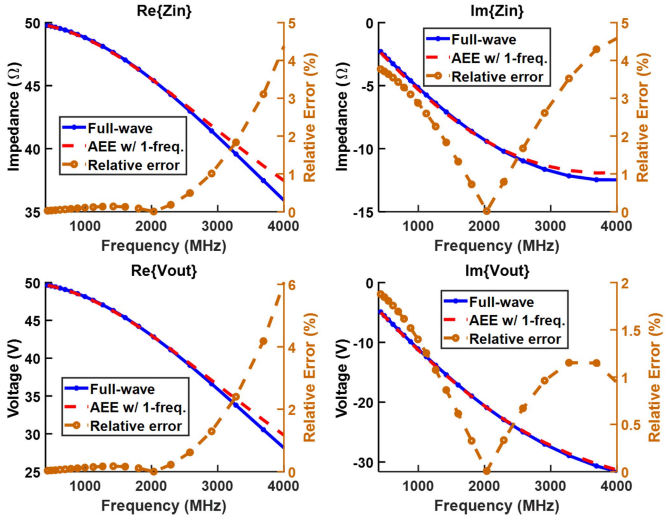

Fig. 5. Quasi-static AEE using a single frequency at 2 GHz versus the full-wave analysis for test problem 1. Top: real and imaginary parts of the input impedance. Bottom: real and imaginary parts of the output voltage.

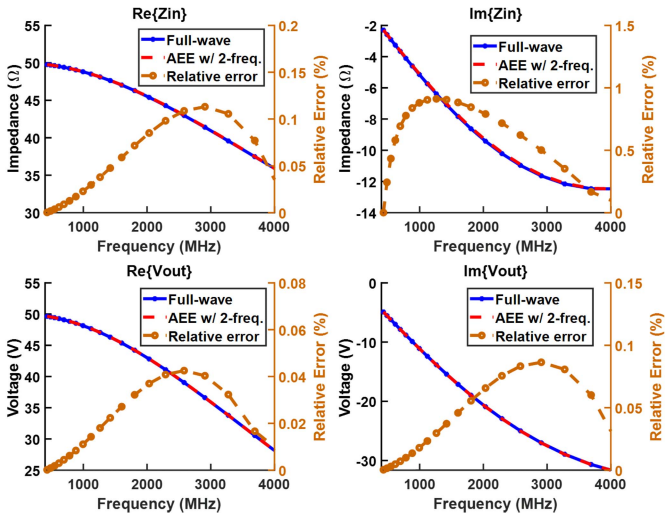

Fig. 6. Quasi-static AEE using two frequencies (400 MHz and 4 GHz) versus the full-wave analysis for test problem 1. Top: real and imaginary parts of the input impedance. Bottom: real and imaginary parts of the output voltage.

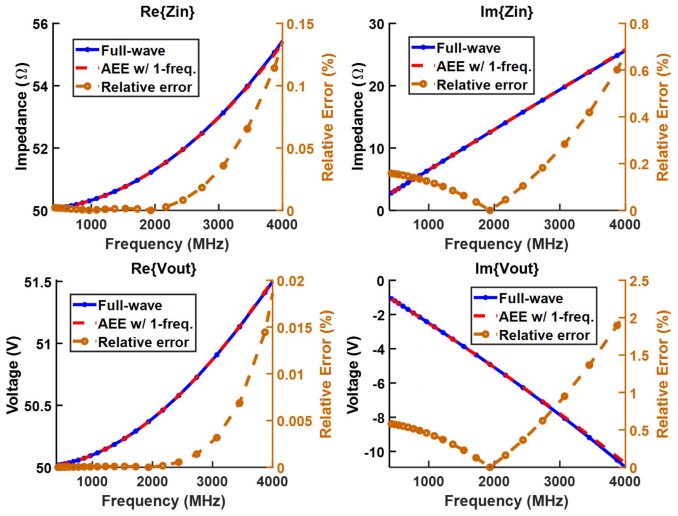

Fig. 7. Quasi-static AEE using a single frequency at 2 GHz versus the full-wave analysis for test problem 2. Top: real and imaginary parts of the input impedance. Bottom: real and imaginary parts of the output voltage.

part is negative, they are capacitively dominant and can be approximated by (18).

Fig. 5 shows the input impedance and output voltage of the quasi-static AEE for test problem 1 using a single frequency at 2 GHz. The results are compared with the full-wave analysis. The relative errors in the quasi-static analysis calculated using the full-wave solution as the reference are also plotted. The maximum error is around 6%. Fig. 6 shows the results in which two frequency points at 400 MHz and 4 GHz are used to include the effect of both inductance and capacitance via (16). A much better agreement is achieved where the maximum error is reduced to about 0.8%. The error remains to be less than 1% for frequencies up to 5 GHz, at which the device's electrical size is about one tenth of the wavelength, and the error gradually increases to 6% at 10 GHz, at which the device's electrical size is about one fifth of the wavelength. The choice of the sampling frequencies is found to be noncritical in the AEE as long as the frequencies are sufficiently apart. For the one-frequency case, the obvious choice is the central frequency. For the case with two sampling frequencies, they can be chosen either at the beginning and end of the frequency band or 25% away from the two ends.

Figs. 7 and 8 show the input impedance and output voltage of the quasi-static AEE versus the full-wave analysis for test problem 2, respectively. As can be seen, the maximum error using the single 2-GHz frequency point is around 2.1%, which is reduced to 0.22% by using two frequency points at 400 MHz and 4 GHz.

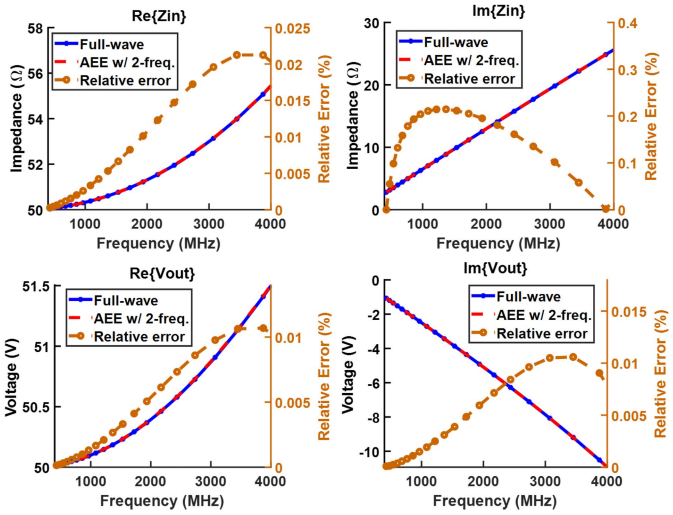

Fig. 8. Quasi-static AEE using two frequencies (400 MHz and 4 GHz) versus the full-wave analysis for test problem 2. Top: real and imaginary parts of the input impedance. Bottom: real and imaginary parts of the output voltage.

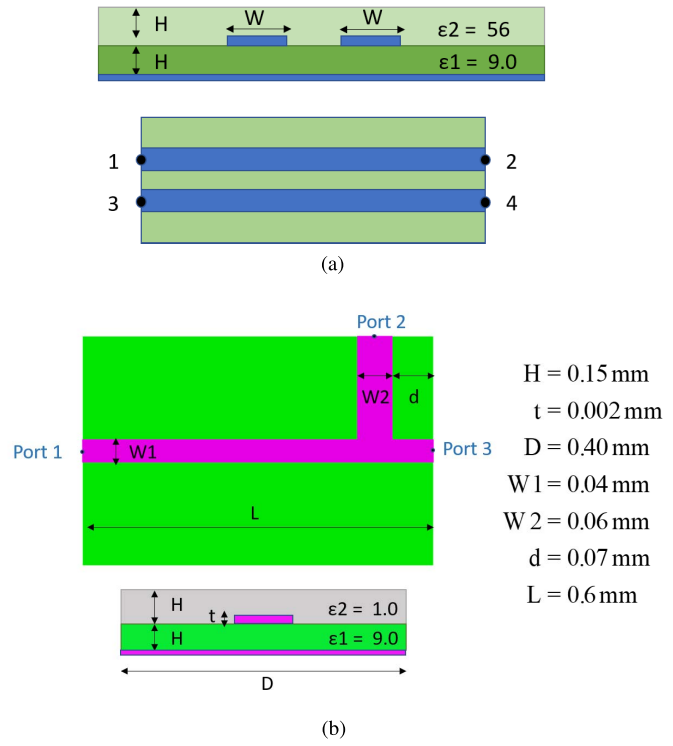

Fig. 9. Test problems for multiport circuits. (a) Test problem 3 (W = 0.04 mm, H = 0.15 mm, T = 0.002 mm, S = 0.04 mm, total width = 0.52 mm, and total length = 1.00 mm). (b) Test problem 4 consisting of one piece of conductor and three ports.

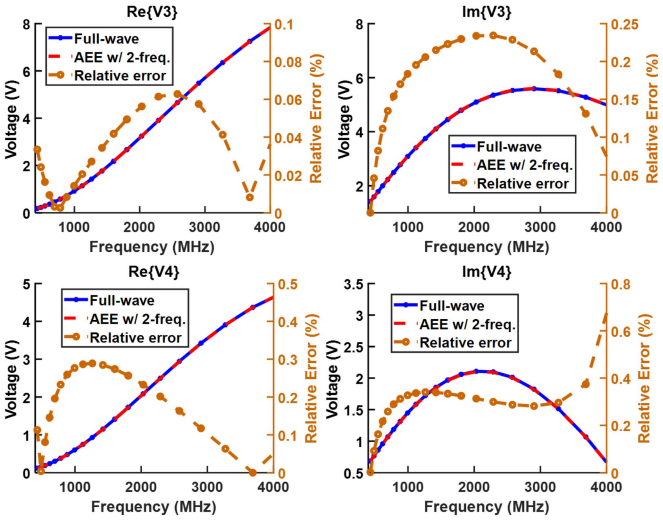

Fig. 10. Quasi-static AEE using two frequencies (400 MHz and 4 GHz) versus the full-wave analysis for test problem 3. Top: voltage at port 3. Bottom: voltage at port 4.

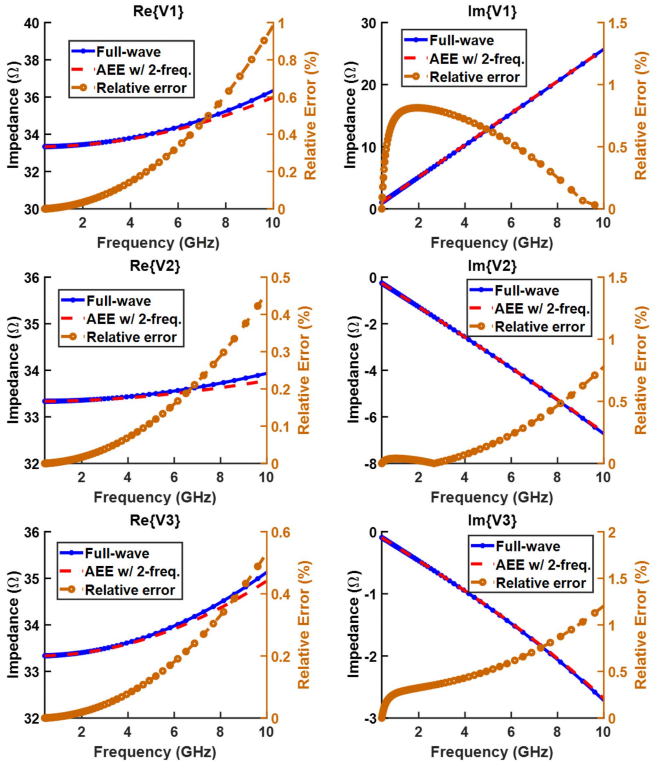

Fig. 11. Quasi-static AEE using two frequencies (400 MHz and 10 GHz) versus the full-wave analysis for test problem 4. From top to bottom: real and imaginary parts of the voltage at ports 1–3.

B. Quasi-Static AEE for Multiport Circuits

Next, we examine the quasi-static AEE for multiport circuits. For this, two test problems are designed. The first is similar to test problem 1, but with two conducting strips separated at a distance of $S = 0.04$ mm, as shown in Fig. 9(a). With a 1.0-A current source applied at port 1 and a 50-Ω resistor applied at the other three ports, the voltages observed at ports 3 and 4 due to mutual coupling are plotted in Fig. 10. Two frequencies at 400 MHz and 4 GHz are selected to perform the quasi-static AEE. The agreement between the quasi-static and full-wave results is excellent over the interested frequency range.

The second test problem consists only one piece of conductor but has three ports, as shown in Fig. 9(b). Port 1 is excited by a 1.0-A current source, and ports 2 and 3 are loaded with a 50- and 100-Ω resistor, respectively. The entire

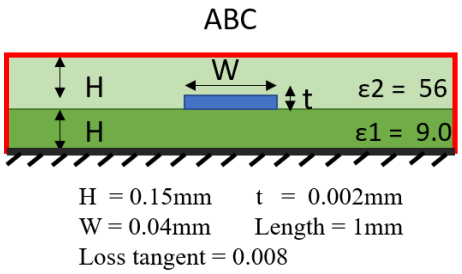

Fig. 12. Test example with a dielectric loss and ABC applied.

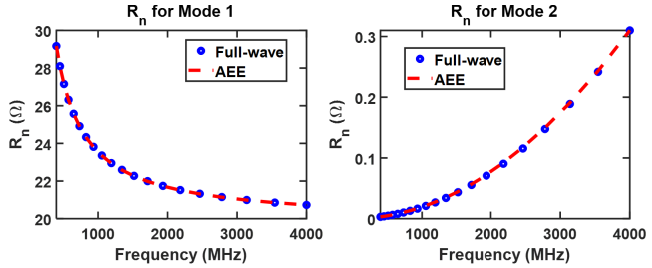

Fig. 13. Characteristic resistance versus frequency for lossy test problem 1 where an ABC is applied and a loss tangent of 0.008 is set in both layers.

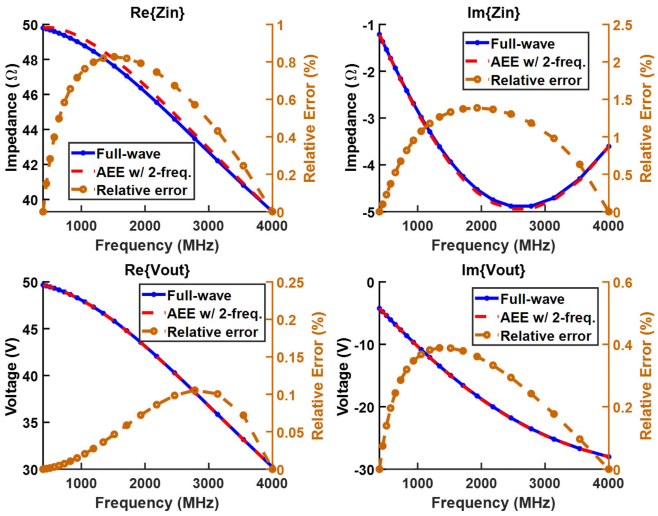

Fig. 14. Quasi-static AEE using two frequencies (400 MHz and 4 GHz) versus the full-wave analysis for the lossy test problem 1 with an ABC and a loss tangent of 0.008. Top: real and imaginary parts of the input voltage. Bottom: real and imaginary parts of the output voltage.

device is enclosed in a perfectly conducting box with a dimension of 0.8 mm × 0.6 mm × 0.3 mm, and the desired frequency range for the analysis is from 400 MHz to 10 GHz. The voltages at the three ports are compared between the quasi-static and full-wave results in Fig. 11, which again shows an excellent agreement with a maximum error of 1.3% at 10 GHz. The accuracy of the two test problems indicates that the quasi-static AEE can correctly and accurately model the multiport RF circuits.

C. Quasi-Static AEE With Dielectric Losses and Absorbing Boundary Condition

All the previous examples use the PEC boundary conditions to truncate the computational domain, and the dielectrics are assumed to be lossless. To extend the proposed AEE to handle lossy cases, we now consider a problem where the dielectric is lossy. We still use the configuration in test problem 1 described in Section III-A, except that the dielectrics have a loss tangent of $\tan\delta = \varepsilon''/\varepsilon' = 0.008$ in both layers. In this case, the real part of the resulting Z-matrix is no longer negligible, and after eigenvalue decomposition, the eigenvalues contain the characteristic resistance R_n.

Different from the characteristic inductance L_n and capacitance C_n whose values remain constant over the frequency band, the resistance R_n is frequency dependent. However, the behavior of R_n versus frequency can be determined based on *a priori* knowledge. For dielectric losses, the loss tangent can be represented by an equivalent conductivity $\sigma_{\text{eq}} = \omega\varepsilon' \tan\delta$, which is a linear function of frequency. Thus, the resistance varies as $R_n \sim R_{\text{const}}/f$. For the radiation loss due to the application of an absorbing boundary condition (ABC) or an impedance boundary condition (IBC) to truncate the computational domain, a simple analysis of the radiated power indicates that the corresponding characteristic resistance R_n is independent of frequency.

Now, we consider test example 1 with both dielectric loss and ABC applied, as shown in Fig. 12. The values of R_n for the two modes are shown in Fig. 13. The resistance R_n in the first mode behaves as $R_n \sim K_1/f + K_2$, where the K_1/f term comes from the dielectric loss and the constant term K_2 is contributed by the ABC. The loss for mode 2 is very small and has a negligible contribution to the total response. By selecting two frequencies at 400 MHz and 4 GHz, L_n and C_n can be calculated from the imaginary part of the nth eigenvalue, and the coefficients K_1 and K_2 for R_n can be obtained from the real part of the eigenvalue.

Fig. 14 compares the results between the quasi-static AEE and full-wave analysis and the relative error is below 1% except for the imaginary part of the input impedance whose absolute value is small. We note that in the case, there are more than two loss mechanisms and the user has no priori knowledge about these losses; two sampling frequency points are not sufficient to determine the frequency-dependent resistances accurately. In this case, one has to either use three frequencies or model only significant losses. For example, in the absence of the radiation loss for a shielded circuit, one can assume that $R_n \approx K \cdot f^{\beta}$ and use the eigenvalues at the two frequencies to determine constants K and β. This, however, is not a critical issue for practical applications because RF circuits are always designed to minimize undesired losses.

D. Numerical Modeling of an SAW Filter

In this section, we construct a very simple design of an SAW filter to illustrate the application of the quasi-static AEE. The input and output layouts are chosen to be the same square-shaped, as shown in Fig. 15. As for the SAW part, it consists of two interdigitated transducers (IDTs) with

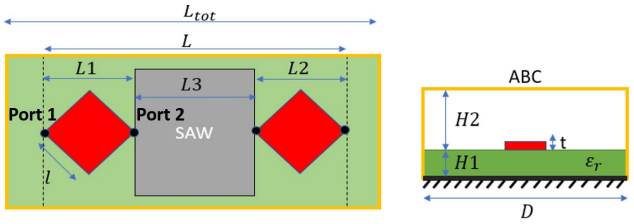

Fig. 15. Simple SAW filter to test the quasi-static and full-wave analyses. (a) Top view of the geometry ($L1 = L2 = 1.41$ mm, $L3 = 3.17$ mm, $l = 1.0$ mm, and $L_{tot} = 7.6$ mm). (b) Side view ($H1 = 0.15$ mm, $H2 = 0.60$ mm, $D = 5.5$ mm, $t = 0.008$ mm, $\epsilon_r = 9.6$, and $\tan\delta = 0.008$.).

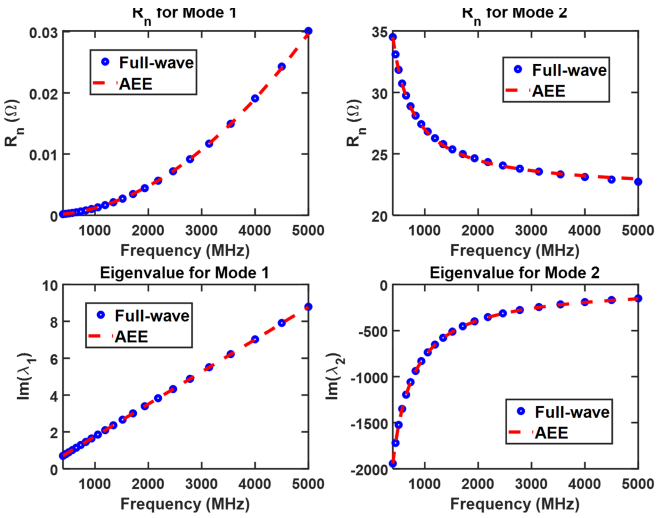

Fig. 16. Real (top) and imaginary (bottom) parts of the eigenvalues of the layout for the SAW filter example.

uniform finger spacing and constant finger overlap, which forms a coupled-resonator filter [41], [42]. Note that we are not concerned with the performance of the filter, and the objective is simply to compare the quasi-static AEE approach with the full-wave analysis. In the quasi-static analysis, we first perform the AEE to approximate the Z-parameters of the input and output layouts. The SAW resonator is modeled as a lumped network characterized by a Y-matrix using the analytical formula in [43]–[45]. By cascading the three Z-matrices, the characteristics of the entire device can be modeled. In the full-wave analysis, the entire filter is modeled using the FEM and the SAW resonator is still modeled as a lumped network and incorporated into the FEM analysis to perform a wave-circuit cosimulation [33]. The substrate material is assumed to be lossy with a dielectric loss tangent of 0.008. The entire structure is enclosed by a truncation boundary where the first-order ABC is applied.

The real and imaginary parts of the eigenvalues for the input and output layouts are plotted in Fig. 16 for the two decomposed eigenmodes. As discussed in Section II, the characteristic resistance R_n consists of two frequency-dependent terms: $R_n \sim K_1/f + K_2$, where the constant comes from the ABC and the term that is inversely proportional to the frequency is introduced by the dielectric loss. After extracting R_n, L_n, and C_n of the layout from sampling frequencies at

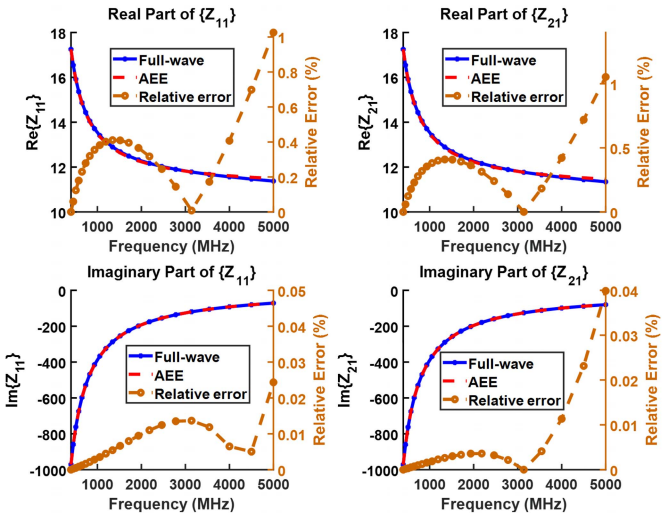

Fig. 17. Z-parameters of the layout for the SAW filter example. Left: Z_{11}. Right: Z_{21}. Because of geometrical symmetry, $Z_{22} = Z_{11}$, and because of reciprocity, $Z_{12} = Z_{21}$.

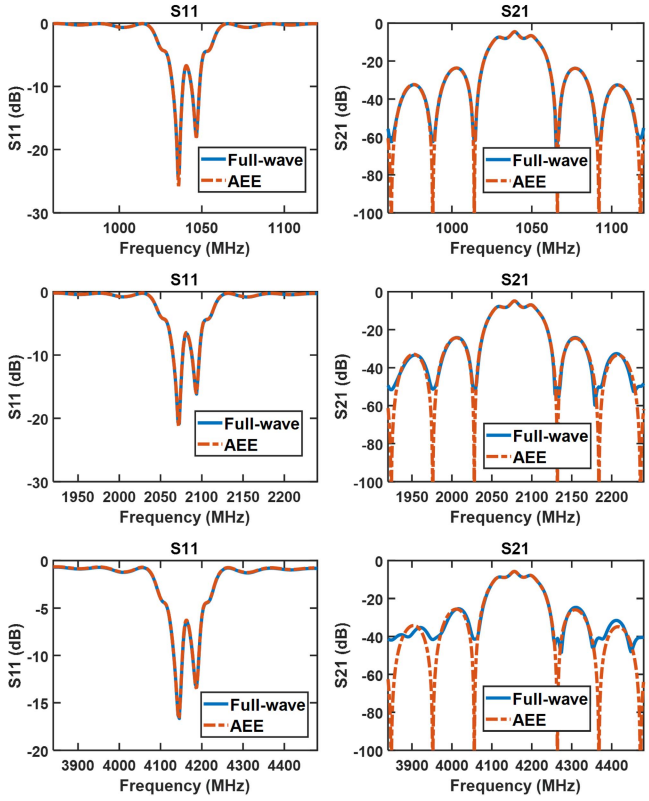

Fig. 18. Quasi-static and full-wave simulated S-parameters centered at three different frequencies for the SAW filter example. From top to bottom, the center frequency is 1040, 2080, and 4160 MHz.

400 and 3140 MHz, the Z-parameters can be approximated over the frequency range of interest, which are given in Fig. 17. By cascading the three segments, the characteristics of the entire device can be calculated, and the comparison with the full-wave analysis centered at three different frequencies is shown in Fig. 18. It can be seen that the agreement between the quasi-static and full-wave results is excellent at the first

three cases, and in the last case, there is a 1-dB discrepancy in S_{21} around the -35-dB level, which is due to the wave effect at the high frequency. For these three simulations, the quasi-static AEE is 50 times faster than the direct full-wave analysis because it extracts the Z-parameters of the input and output layouts only at two selected frequencies and the circuit analysis time is negligible, whereas the full-wave analysis has to be carried out at every frequency point and the frequency sampling points have to be dense enough to capture drastic variations in the frequency responses of the filter.

IV. Conclusion

A new fast frequency sweep method based on AEE has been proposed an efficient analysis of miniature passive RF circuits. In this approach, the Z-parameters are first extracted at one or two sampling frequencies using a full-wave simulation. The eigenvalue decomposition is then performed to diagonalize the impedance matrix. The analytic extension is applied to extend the eigenvalues from the sampling frequencies to all other frequencies via a functional equation. The Z-parameters or Y-parameters can finally be evaluated from their expansion using eigenvectors. For miniature RF circuits, the characteristic capacitance and inductance in each eigenvalue and the corresponding eigenvector are frequency independent, whereas the frequency dependence in the characteristic resistance can be predetermined. The accuracy of this quasi-static AEE has been investigated by comparing its solution with that of the full-wave analysis based on the solution of Maxwell's equations. In the numerical examples, a comparison between the one- and two-frequency approximations was first presented. It has been shown that for some applications where the device is electrically very small, one-frequency approximation can provide acceptable accuracy. A second frequency can be added to further improve accuracy. The modeling of losses introduced by dielectric losses and ABCs has also been discussed, and the frequency behaviors of the corresponding characteristic resistances have been studied. It has been found that the quasi-static AEE is very accurate (with a relative error less than 1%) within the quasi-static range where the circuit components are smaller than one tenth of the effective wavelength and it remains reasonably accurate with a relative error less than 6% when the sizes of the circuit components increase to one fifth of the effective wavelength. In conclusion, the proposed AEE provides a fast frequency sweep for the analysis of RF circuits, and it yields both a mathematical expansion of the Z- or Y-parameters and a physical LEC model. The method can be further extended to high frequencies by considering the frequency dependence of the modal capacitances and inductances and eigenvectors and thus removing its limitation to quasi-static applications.

References

[1] A. E. Ruehli, "Equivalent circuit models for three-dimensional multiconductor systems," *IEEE Trans. Microw. Theory Techn.*, vol. 22, no. 3, pp. 216–221, Mar. 1974.

[2] R. Mittra, W. D. Becker, and P. H. Harms, "A general purpose Maxwell solver for the extraction of equivalent circuits of electronic package components for circuit simulation," *IEEE Trans. Circuits Syst. I, Fundam. Theory Appl.*, vol. 39, no. 11, pp. 964–973, 1992.

[3] T. Mangold and P. Russer, "Full-wave modeling and automatic equivalent-circuit generation of millimeter-wave planar and multilayer structures," *IEEE Trans. Microw. Theory Techn.*, vol. 47, no. 6, pp. 851–858, Jun. 1999.

[4] L. Zhu and K. Wu, "Field-extracted lumped-element models of coplanar stripline circuits and discontinuities for accurate radiofrequency design and optimization," *IEEE Trans. Microw. Theory Techn.*, vol. 50, no. 4, pp. 1207–1215, Apr. 2002.

[5] G. J. Burke, E. K. Miller, S. Chakrabarti, and K. Demarest, "Using model-based parameter estimation to increase the efficiency of computing electromagnetic transfer functions," *IEEE Trans. Magn.*, vol. 25, no. 4, pp. 2807–2809, Jul. 1989.

[6] K. Kottapalli, T. K. Sarkar, Y. Hua, E. K. Miller, and G. J. Burke, "Accurate computation of wide-band response of electromagnetic systems utilizing narrow-band information," *IEEE Trans. Microw. Theory Techn.*, vol. 39, no. 4, pp. 682–687, Apr. 1991.

[7] L. T. Pillage and R. A. Rohrer, "Asymptotic waveform evaluation for timing analysis," *IEEE Trans. Comput.-Aided Design Integr. Circuits Syst.*, vol. 9, no. 4, pp. 352–366, Apr. 1990.

[8] M. A. Kolbehdari, M. Srinivasan, M. S. Nakhla, Q.-J. Zhang, and R. Achar, "Simultaneous time and frequency domain solutions of EM problems using finite element and CFH techniques," *IEEE Trans. Microw. Theory Techn.*, vol. 44, no. 9, pp. 1526–1534, 1996.

[9] M. Li, Q. J. Zhang, and M. Nakhla, "Finite difference solution of EM fields by asymptotic waveform techniques," *IEE Proc.-Microw., Antennas Propag.*, vol. 143, no. 6, pp. 512–520, Dec. 1996.

[10] P. Feldmann and R. W. Freund, "Efficient linear circuit analysis by pade approximation via the lanczos process," *IEEE Trans. Comput.-Aided Design Integr. Circuits Syst.*, vol. 14, no. 5, pp. 639–649, May 1995.

[11] M. Celik and A. C. Cangellaris, "Simulation of dispersive multiconductor transmission lines by Pade approximation via the Lanczos process," *IEEE Trans. Microw. Theory Techn.*, vol. 44, no. 12, pp. 2525–2535, Dec. 1996.

[12] R. Freund, "Reduced-order modeling techniques based on Krylov subspaces and their use in circuit simulation," in *Applied and Computational Control, Signals, and Circuits*, vol. 1, B. N. Datta, Ed. Boston, MA, USA: Birkhäuser, 1999, pp. 435–498.

[13] Z. Bai and R. W. Freund, "A partial Padé-via-Lanczos method for reduced-order modeling," *Linear Algebra Appl.*, vols. 332–334, pp. 139–164, Aug. 2001.

[14] C. K. Aanandan, P. Debernardi, R. Orta, R. Tascone, and D. Trinchero, "Problem-matched basis functions for moment method analysis–An application to reflection gratings," *IEEE Trans. Antennas Propag.*, vol. 48, no. 1, pp. 35–40, Jan. 2000.

[15] F. Bertazzi, O. A. Peverini, M. Goano, G. Ghione, R. Orta, and R. Tascone, "A fast reduced-order model for the full-wave FEM analysis of lossy inhomogeneous anisotropic waveguides," *IEEE Trans. Microw. Theory Tech.*, vol. 50, no. 9, pp. 2108–2114, Sep. 2002.

[16] S.-H. Lee and J.-M. Jin, "Adaptive solution space projection for fast and robust wideband finite-element simulation of microwave components," *IEEE Microw. Wireless Compon. Lett.*, vol. 17, no. 7, pp. 474–476, Jul. 2007.

[17] R. Harrington and J. Mautz, "Theory of characteristic modes for conducting bodies," *IEEE Trans. Antennas Propag.*, vol. AP-19, no. 5, pp. 622–628, Sep. 1971.

[18] R. Harrington, J. Mautz, and Y. Chang, "Characteristic modes for dielectric and magnetic bodies," *IEEE Trans. Antennas Propag.*, vol. AP-20, no. 2, pp. 194–198, Mar. 1972.

[19] M. Cabedo-Fabres, E. Antonino-Daviu, A. Valero-Nogueira, and M. Bataller, "The theory of characteristic modes revisited: A contribution to the design of antennas for modern applications," *IEEE Antennas Propag. Mag.*, vol. 49, no. 5, pp. 52–68, Oct. 2007.

[20] B. D. Raines, "Systematic design of multiple antenna systems using characteristic modes," Ph.D. dissertation, Dept. Elect. Comput. Eng., Ohio State Univ., Columbus, OH, USA, 2011.

[21] J. Ethier, "Antenna shape synthesis using characteristic mode concepts," Ph.D. dissertation, School Elect. Eng. Comput. Sci., Univ. Ottawa, Ottawa, ON, Canada, 2012.

[22] J. J. Adams and J. T. Bernhard, "Broadband equivalent circuit models for antenna impedances and fields using characteristic modes," *IEEE Trans. Antennas Propag.*, vol. 61, no. 8, pp. 3985–3994, Aug. 2013.

[23] Q. Wu, S. Guo, and D. Su, "On the eigenmodes of small conducting objects," *IEEE Antennas Wireless Propag. Lett.*, vol. 13, pp. 1667–1670, 2014.

[24] M. Vogel, G. Gampala, D. Ludick, and C. J. Reddy, "Characteristic mode analysis: Putting physics back into simulation," *IEEE Antennas Propag. Mag.*, vol. 57, no. 2, pp. 307–317, Apr. 2015.

[25] Y. Chen and C.-F. Wang, *Characteristic Modes: Theory and Applications in Antenna Engineering*. Hoboken, NJ, USA: Wiley, 2015.

[26] Q. Wu, W. Su, Z. Li, and D. Su, "Reduction in out-of-band antenna coupling using characteristic mode analysis," *IEEE Trans. Antennas Propag.*, vol. 64, no. 7, pp. 2732–2742, Jul. 2016.

[27] M. Meng and Z. Nie, "Study on characteristic mode analysis of three-dimensional conducting objects in lossless layered medium," *IEEE Access*, vol. 6, pp. 77606–77614, 2018.

[28] W. Su, Q. Zhang, S. Alkaraki, Y. Zhang, X.-Y. Zhang, and Y. Gao, "Radiation energy and mutual coupling evaluation for multimode MIMO antenna based on the theory of characteristic mode," *IEEE Trans. Antennas Propag.*, vol. 67, no. 1, pp. 74–84, Jan. 2019.

[29] Q. Wu, "General metallic-dielectric structures: A characteristic mode analysis using volume-surface formulations," *IEEE Antennas Propag. Mag.*, vol. 61, no. 3, pp. 27–36, Jun. 2019.

[30] T. Dhaene and D. De Zutter, "CAD-oriented general circuit description of uniform coupled lossy dispersive waveguide structures," *IEEE Trans. Microw. Theory Techn.*, vol. 40, no. 7, pp. 1545–1554, Jul. 1992.

[31] G. G. Gentili and M. Salazar-Palma, "The definition and computation of modal characteristic impedance in quasi-TEM coupled transmission lines," *IEEE Trans. Microw. Theory Techn.*, vol. 43, no. 2, pp. 338–343, Feb. 1995.

[32] S. H. Hall and H. L. Heck, *Advanced Signal Integrity for High-Speed Digital Designs*. Hoboken, NJ, USA: Wiley, 2009.

[33] J. M. Jin, *The Finite Element Method in Electromagnetics*, 3rd ed. Hoboken, NJ, USA: Wiley, 2014.

[34] J. B. Manges and Z. J. Cendes, "Tree-cotree decompositions for first-order complete tangential vector finite elements," *Int. J. Numer. Methods Eng.*, vol. 40, no. 9, pp. 1667–1685, May 1997.

[35] S. H. Lee and J. M. Jin, "Application of the tree-cotree splitting for improving matrix conditioning in the full-wave finite-element analysis of high-speed circuits," *Microw. Opt. Tech. Lett.*, vol. 50, no. 6, pp. 1476–1481, 2008.

[36] R. Wang, D. J. Riley, and J.-M. Jin, "Application of tree-cotree splitting to the time-domain finite-element analysis of electromagnetic problems," *IEEE Trans. Antennas Propag.*, vol. 58, no. 5, pp. 1590–1600, May 2010.

[37] R. Silver, "Characteristic mode analysis and analytic continuation of the electromagnetic admittance of SAW devices," Resonant, Goleta, CA, USA, Tech. Rep. 20170815, Aug. 2017.

[38] M. Cabedo, "Systematic design of antennas using the theory of characteristic modes," Ph.D. dissertation, Dept. Comput. Sci. Syst. Eng., Universidad Politechnica de Valencia, Valencia, Spain, 2007.

[39] K. A. Obeidat, B. D. Raines, and R. G. Rojas, "Discussion of series and parallel resonance phenomena in the input impedance of antennas," *Radio Sci.*, vol. 45, no. 6, pp. 1–9, Dec. 2010.

[40] H. R. Stuart, "Eigenmode analysis of a two element segmented capped monopole antenna," *IEEE Trans. Antennas Propag.*, vol. 57, no. 10, pp. 2980–2988, Oct. 2009.

[41] T. M. Reeder and D. K. Winslow, "Characteristics of microwave acoustic transducers for volume wave excitation," *IEEE Trans. Microw. Theory Techn.*, vol. MTT-17, no. 11, pp. 927–941, Nov. 1969.

[42] P. Warder and A. Link, "Golden age for filter design: Innovative and proven approaches for acoustic filter, duplexer, and multiplexer design," *IEEE Microw. Mag.*, vol. 16, no. 7, pp. 60–72, Aug. 2015.

[43] W. R. Smith, H. M. Gerard, J. H. Collins, T. M. Reeder, and H. J. Shaw, "Analysis of interdigital surface wave transducers by use of an equivalent circuit model," *IEEE Trans. Microw. Theory Techn.*, vol. MTT-17, no. 11, pp. 856–864, Nov. 1969.

[44] W. R. Smith, H. M. Gerard, and W. R. Jones, "Analysis and design of dispersive interdigital surface-wave transducers," *IEEE Trans. Microw. Theory Techn.*, vol. MTT-20, no. 7, pp. 458–471, Jul. 1972.

[45] C. K. Campbell, *Surface Acoustic Wave Devices and Their Signal Processing Applications*. San Diego, CA, USA: Academic, 1989.

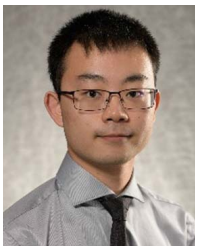

Hongliang Li (Graduate Student Member, IEEE) was born in Luohe, Henan, China, in 1994. He received the B.S. degree in electrical engineering and information science from the University of Science and Technology of China, Hefei, China, in 2017, and the M.S. degree in electrical and computer engineering from the University of Illinois at Urbana–Champaign, Urbana, IL, USA, in 2020, where he is currently pursuing the Ph.D. degree in electrical engineering.

Since 2017, he has been a Research Assistant with the Center for Computational Electromagnetics, University of Illinois at Urbana–Champaign. His research interests include the time- and frequency-domain finite-element methods, numerical modeling of electrical machines and RF circuits, and the development of fast algorithms.

Jian-Ming Jin (Fellow, IEEE) is currently the Y. T. Lo Chair Professor with the Department of Electrical and Computer Engineering and the Director of the Electromagnetics Laboratory and the Center for Computational Electromagnetics. He has authored or coauthored more than 280 articles in refereed journals and 22 book chapters. He has also authored *The Finite Element Method in Electromagnetics* (Wiley, First Edition, 1993, Second Edition, 2002, and Third Edition, 2014), *Electromagnetic Analysis and Design in Magnetic Resonance Imaging* (CRC, 1998), and *Theory and Computation of Electromagnetic Fields* (Wiley, First Edition, 2010 and Second Edition, 2015) and coauthored *Computation of Special Functions* (Wiley, 1996), *Fast and Efficient Algorithms in Computational Electromagnetics* (Artech, 2001), and *Finite Element Analysis of Antennas and Arrays* (Wiley, 2008). His current research interests include computational electromagnetics, multiphysics modeling, scattering and antenna analysis, electromagnetic compatibility, high-frequency circuit modeling and analysis, bioelectromagnetics, and magnetic resonance imaging.

Dr. Jin was elected by the ISI as one of the worlds most cited authors in 2002 and is also a Fellow of the Optical Society of America, the Electromagnetics Academy, and the Applied Computational Electromagnetics Society (ACES). He was a recipient of the 1994 National Science Foundation Young Investigator Award, the 1995 Office of Naval Research Young Investigator Award, the 1999 ACES Valued Service Award, the 2014 ACES Technical Achievement Award, the 2015 IEEE APS Chen-To Tai Distinguished Educator Award, the 2015 and 2020 IEEE Edward E. Altschuler AP-S Magazine Prize Paper Awards, the 2016 ACES Computational Electromagnetics Award, the 2017 IEEE APS Harrington-Mittra Computational Electromagnetics Award, and the 2020 ECE Distinguished Educator Award from the University of Michigan. He was awarded Adjunct, Visiting, Guest, or Chair Professorship by 14 institutions around the world and appointed as an IEEE AP-S Distinguished Lecturer in 2015. He was a recipient of the 1997 and 2000 Xerox Research Awards and was appointed as the first Henry Magnuski Outstanding Young Scholar in 1998 and later as a Sony Scholar in 2005 at the University of Illinois at Urbana–Champaign. His name appeared 24 times in the University's List of Excellent Instructors. His students have received the best paper awards in IEEE 16th Topical Meeting on Electrical Performance of Electronic Packaging and 25th, 27th, 31st, and 32nd Annual Review of Progress in Applied Computational Electromagnetics. He was an Associate Editor and a Guest Editor of the IEEE TRANSACTIONS ON ANTENNAS AND PROPAGATION, *Radio Science*, *Electromagnetics*, *Microwave and Optical Technology Letters*, and *Medical Physics*. He serves as the Editor-in-Chief for *International Journal of Numerical Modeling: Electronic Networks, Devices and Fields*.

Douglas R. Jachowski (Member, IEEE) received the B.S. and M.S. degrees in electrical engineering from Stanford University, Stanford, CA, USA, in 1981 and 1987, respectively.

From 1982 to 1987, he designed circuits, instruments, and integrated sensors at MEMS pioneers Transensory Devices and NovaSensor, both of Fremont, CA. While moonlighting in 1984, he codeveloped the first self-tuning transmitter combiner. From 1988 to 1994, as the Director of filter technology for Allen Telecom, Reno, NV, USA, he designed microwave filters for cell phone base stations and pioneered the use of dielectric resonators in commercial applications. Following a period as a consultant, he joined the Naval Research Laboratory (NRL), Washington, DC, USA, in 2003, where his research focused on absorptive and tunable filters and reconfigurable receiver front ends. He was the Head of the Solid-State Circuits Section, NRL from 2009 to 2012 before returning to consulting. In 2016, he joined Resonant Inc., Goleta, CA, where he designs SAW and BAW multiplexers and works to improve acoustic-wave filter technology and design techniques.

Robert B. Hammond (Life Member, IEEE) received the B.S., M.S., and Ph.D. degrees in physics and applied physics from Caltech, Pasadena, CA, USA, in 1971, 1972, and 1976, respectively.

Under thesis advisors J. W. Mayer and T. C. McGill, he measured for the first time the thermodynamic properties of the electron-hole-liquid in silicon and the splitting of the silicon exciton ground state. From 1976 to 1987, he was with the Los Alamos National Laboratory, Los Alamos, NM, USA, where he led Electronics Research and Exploratory Development and established a semiconductor physics and device development group. He led the development of a variety of novel materials, devices, and instruments, including subnanosecond radiation detectors and multigigawatt switches, subpicosecond electrical characterization measurements, and laser position sensors and beam diagnostics. He contributed to the understanding of the fundamental mechanisms of pulsed laser annealing in silicon and the fundamental properties of highly excited silicon at low temperature. In 1987, he co-founded Superconductor Technologies Inc., Santa Barbara, CA, where he was the Chief Technical Officer in 2012. At STI, he built a team of engineers and scientists, lead technology development, and directed corporate technology strategy and intellectual property. He participated in raising >$250M in investment capital, led the company for the two years preceding its successful IPO in 1993, and attracted and successfully executed against >$100M in DARPA technology development funding. Under his leadership, STI pioneered the development and manufacturing of superconducting TlBaCaCuO and YBaCuO thin films, superconducting wireless microwave filter chips, and a no-maintenance Stirling cryocooler, all incorporated in STIs flagship product SuperLink. These RF front-end systems ultimately operated 24/7 in 7000 cellular base stations across USA. In 2012, he cofounded Resonant Inc., Goleta, CA, USA, where he is currently the Chief Technical Officer. Resonant designs SAW and BAW filters and multiplexers for RF front-end applications in smartphones. Resonant recently invented a new acoustic filter technology, XBAR, that promises to address the many novel emerging requirements for RFFE filtering in 5G smartphones. He has authored hundreds of technical articles and holds several dozen patents.